DOI: 10.1002/ejic.200600726

Reactivity and X-ray Structural Studies in Ligand Substitution of [Cp/(Ind)Ru(dppf)Cl] – Epimerisation in [Cp/(Ind)Ru(Josiphos)Cl] {Cp = η^5-C_5H_5, Ind = η^5-C_7H_9, dppf = 1,1′-Bis(diphenylphosphanyl)ferrocene, Josiphos = (*R*)-(–)-1-[(*S*)-2-(Diphenylphosphanyl)ferrocenyl]ethyldicyclohexylphosphane}

Sin Yee Ng,[a] Guihua Fang,[a] Weng Kee Leong,*[a] Lai Yoong Goh,*[a] and Marc V. Garland[b]

Keywords: Indenyl / Ruthenium / dppf / Josiphos / Epimerisation / Phosphanes

Ligand substitution of [(Ind)Ru(PPh_3)$_2$Cl] (**1**) led to the isolation of [(Ind)Ru(PPh_3){$Ph_2P(CH_2)_2C_9H_7$}Cl] (**2**), [(Ind)Ru(dppf)Cl] (**3**) and [(Ind)Ru{$(Ph_2PCH_2)_3CMe$}]PF_6 ([**4**]PF_6), and diastereoisomers [(*R*)- and (*S*)-(Ind)Ru(Josiphos)Cl] [(*R*)-**5** and (*S*)-**5**], where (*R*)-(*S*)-Josiphos is the ferrocene-based chiral diphosphane ligand (*R*)-(–)-1-[(*S*)-2-(diphenylphosphanyl)ferrocenyl] ethyldicyclohexylphosphane. The Cp analogues of **5**, viz. (*R*)-**6** and (*S*)-**6**, were also obtained from [CpRu(PPh_3)$_2$Cl] (**1a**). Josiphos-dependent epimerisation was observed, with conversion of the (*S*) isomer to the (*R*) isomer in both cases. Chloride abstraction of **3** with $NaPF_6$ in CH_3CN and NaN_3 in EtOH gave [(Ind)Ru(dppf)(CH_3CN)]PF_6 ([**7**]PF_6) and [(Ind)Ru(dppf)(N_3)] (**8**), respectively. The azido ligand in **8** underwent [3+2] dipolar cycloaddition with dimethyl acetylenedicarboxylate to give a *N*-bound bis(methoxycarbonyl)-1,2,3-triazolato complex, **9**. X-ray crystal structures of the new complexes, except (*R*)-**5**, (*S*)-**5** and (*S*)-**6**, have been determined.

Introduction

The chemistry of phosphane organometallic complexes has been well established in the last four decades,[1] interest being fuelled by their roles in medicinal and catalytic applications.[2] In particular, [CpRu(PPh_3)$_2$Cl] (**1a**), first synthesised in 1969 by Gilbert and Wilkinson,[3] has attracted much attention. A rich chemistry has unfolded, based on the facile substitution of the PPh_3 ligand by two-electron donors, as well as the ready displacement of the chlorido ligand by both anionic and neutral ligands.[4] Its well-defined CpRu(PPh_3)$_2$ moiety is an attractive auxiliary that can be used for the attachment of organic groups in studies of their steric and electronic effects on the chemical[4a] and catalytic[5] reactivity of the complex. More recently, the role of metallophosphane ligands, for example, of the symmetrical and unsymmetrical ferrocenyl type, in catalysis of organic reactions is increasingly being studied, as the ligands become more readily available.[6]

The marked effect of the capping ligand on reactivity of the complex came to light with the synthesis of [(Ind)Ru(PPh_3)$_2$Cl] (**1**) (Ind = η^5-C_9H_7) some 16 years after that of its Cp analogue, **1a**.[7] The enhanced reactivity, commonly known as the "indenyl effect", was found to be largely brought about by ring slippage.[8] The combined effect of capping ligand and phosphane ligand variant would therefore be of interest. We note that research in recent years on (Ind)Ru chemistry has been focused on vinylidene and allenylidene complexes by the group of Gimeno,[8,9] and nitrogen-containing ligands, for example, amines, nitriles, *N*,*N*′-donor Schiff bases and azine ligands, by Kollipara and co-workers.[10] In this work, we have investigated the reactivity of **1** with the ferrocenyl diphosphane ligands 1,1′-bis(diphenylphosphanyl)ferrocene (dppf) and chiral ferrocenyl diphosphane ligand {(*R*)-(*S*)-Josiphos} and with the tripod ligand {$(Ph_2CH_2)_3CMe$}, and the reactivity of [(Ind)Ru(dppf)Cl] (**3**) towards N-containing ligands.

Results and Discussion

Phosphane Substitution

Synthesis of [(Ind)Ru(PPh_3){$Ph_2P(CH_2)_2C_9H_7$}Cl] (2), [(Ind)Ru(dppf)Cl] (3) and [(Ind)Ru(tripod)]PF_6 ([4]PF_6)

As in [CpRu(PPh_3)$_2$Cl] (**1a**), the substitution lability of PPh_3 in [(Ind)Ru(PPh_3)$_2$Cl] (**1**) has provided an easy entry to various [(Ind)Ru] complexes. For instance, [(Ind)Ru(diphos)Cl] had been synthesised from a reaction of [(Ind)-

[a] Department of Chemistry, National University of Singapore, 3 Science Drive, Singapore 117543
Fax: +65-6779-1691
E-mail: chmgohly@nus.edu.sg
chmlwk@nus.edu.sg
[b] Institute of Chemical and Engineering Sciences, 1 Pesek Road, Jurong Island, Singapore 627833

$Ru(PPh_3)_2Cl$] by substitution with the desired diphos in refluxing toluene.[7] Adopting the reported procedure for the synthesis of (Ind)Ru(dppe)Cl [dppe = 1,2-bis(diphenylphosphanyl)ethane],[11] phosphane substitution of **1** at elevated temperature in toluene gave air- and moisture-stable red solids of the monophosphane-substituted complex [(Ind)-$Ru\{Ph_2P(CH_2)_2C_9H_7\}(PPh_3)Cl$] (**2**), containing the (1-indenylethyl)diphenylphosphane ligand **LH** (Scheme 1a), the diphosphane-substituted complex [(Ind)Ru(dppf)Cl] (**3**) with dppf (Scheme 1b), and a totally substituted complex [(Ind)-$Ru(Ph_2PCH_2)_3Me]PF_6$ ([**4**]PF_6) with the tripodal triphos ligand $(Ph_2PCH_2)_3CMe$ (Scheme 1c), in high yields.

It is anticipated that phosphane substitution of **1** will be facilitated by the release of steric stress in the coordination sphere by dissociation of one or both of the bulky PPh_3 ligands. This is very likely the driving force in the formation of **2**, as the ligand **LH** is less bulky than PPh_3. In the cases of **3** and [**4**]PF_6, the reactions are additionally assisted by the chelating effect of the incoming di- and triphosphane ligand, respectively.

The ^1H NMR spectrum of **2** shows four multiplets in the range δ = 1.79–3.52, assigned to the four inequivalent methylene protons of **LH**. The CH_2 protons of the five-membered ring of **LH** resonate at δ = 2.93, while the olefinic proton resonates at a higher field at δ = 6.5. On the other hand, the protons H^{1-3} (see Experimental Section for numbering scheme) of the η^5-coordinated Ind ligand resonate at δ = 4.95–5.00 and δ = 5.78 ppm. The ^{31}P NMR spectrum shows two doublets at δ = 46.5 and δ = 50.0 with $^2J_{PP}$ = 42.9 Hz due to the coupling of the two inequivalent phosphorus atoms.

The ^1H NMR spectrum of **3** shows an ABCD pattern for the proton signals of the ferrocene rings at δ = 3.66, 3.83, 3.90 and 4.20, suggesting an eclipsed conformation for the chelating dppf ligand in **3**;[12] this was supported by the X-ray single-crystal diffraction analysis. The Cp proton signals of the η^5-indenyl ligand appear at δ = 4.66 (H^1) and 5.57 ($H^{2,3}$). The latter resonance is 1.67 ppm downfield shifted from that in the bis(PPh_3) analogue, owing to relief from the shielding effect caused by the ring current of the Ph ring of PPh_3 on H^2 and H^3 in **1**.[13]

The ^1H NMR spectrum of [**4**]PF_6 shows a multiplet at $\delta \approx 1.5$ and a broad singlet at $\delta \approx 2.39$, assigned to the methyl and methylene groups of the tripod ligand, indicating the fluxionality of these groups in solution. However, a sharp singlet at δ = 39.9 in the ^{31}P NMR spectrum indicates an equivalent chemical environment for the three coordinated phosphorus atoms of tripod. The proton resonances of H^1 and $H^{2,3}$ of the indenyl ligand appear at δ = 5.51 and 5.57 ppm, while H^{4-7} appear as two characteristic four-line multiplets at δ = 7.31–7.34 and δ = 7.43–7.47, respectively.

The molecular structures of **2**, **3** and [**4**]$^+$ have been determined by single-crystal X-ray crystallographic studies; their ORTEP diagrams are shown in Figures 1, 2 and 3, respectively, and selected bond parameters are compared with those of CpRu(dppf)Cl[14] in Table 1.

The molecular structures of **2** and **3** show Ru hexacoordinated to Ind, a Cl atom and two phosphorus atoms, that is, from PPh_3 and $C_9H_7(CH_2)_2PPh_2$ in **2** and from chelating dppf in **3**. The molecular structure of [**4**]$^+$ consists of a mononuclear cation [(η^5-Ind)Ru(tripod)]$^+$ and PF_6^- anion, to-

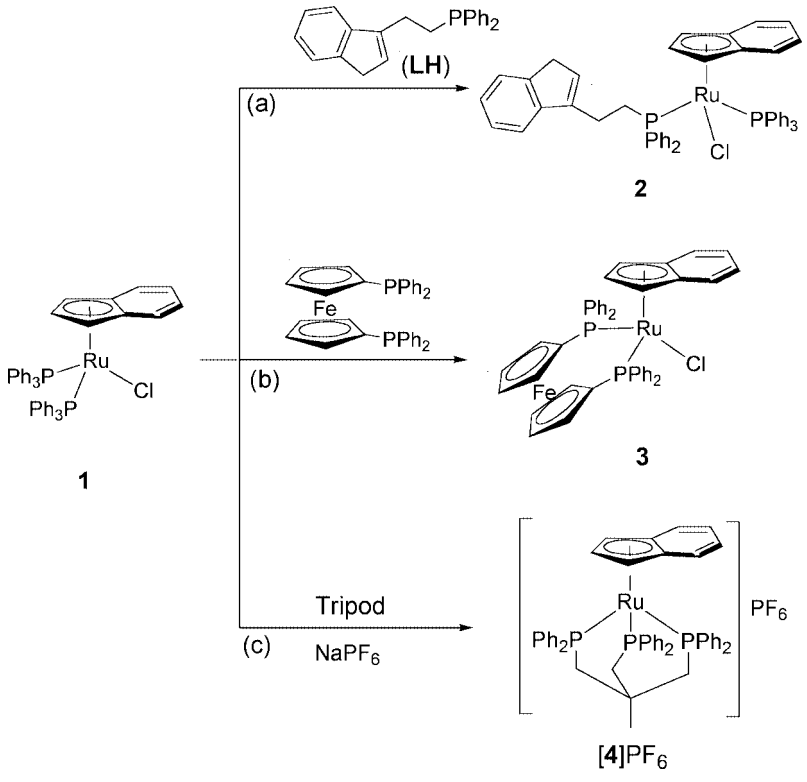

Scheme 1.

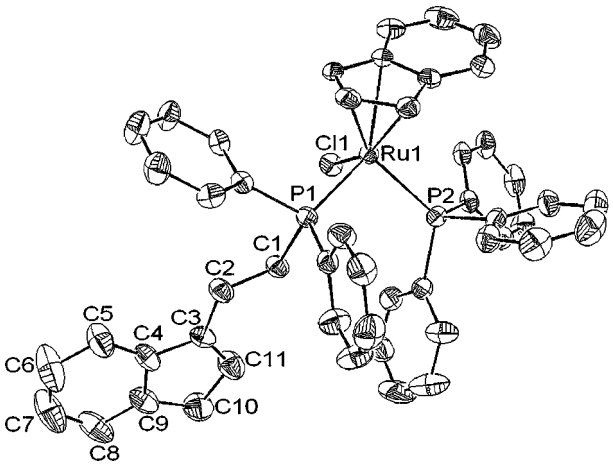

Figure 1. ORTEP diagram of **2**. Thermal ellipsoids are drawn to 50% probability level. Hydrogen atoms are omitted for clarity. Selected bond lengths: C1–C2 1.530(7) Å; C2–C3 1.506(6) Å; C3–C11 1.329(7) Å; C3–C4 1.454(7) Å; C4–C5 1.375(7) Å; C5–C6 1.388(8) Å; C6–C7 1.374(9) Å; C7–C8 1.368(9) Å; C8–C9 1.3859(8) Å; C9–C4 1.401(7) Å; C9–C10 1.513(8) Å; C10–C11 1.494(7) Å. Other bond parameters are given in Table 1.

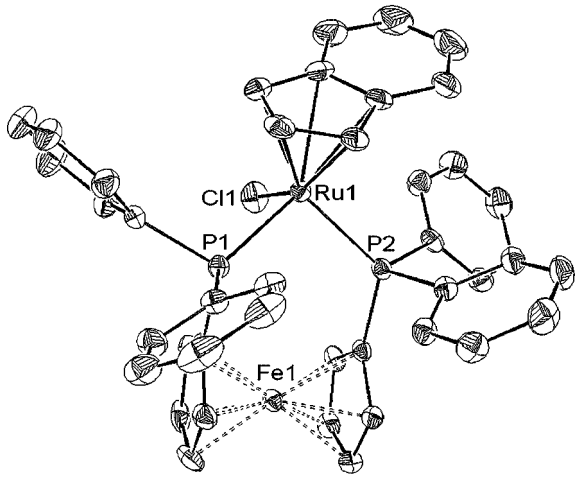

Figure 2. ORTEP diagram of **3**. Thermal ellipsoids are drawn to 50% probability level. Hydrogen atoms are omitted for clarity.

gether with two solvent molecules of dichloromethane, one of which is disordered.

A general, yet prominent structural feature of η^5-indenyl complexes is the distortion from η^5- to η^3-coordination, equivalent to an allyl-ene bonding description for the C_5 ring. Such a distortion is found in **2**, **3** and [**4**]$^+$, as evident from the values of their slip distortions (Δ) and hinge angles (HA), which fall in the range of small or moderate distortion towards a η^3 binding mode.[15] The slightly larger distortion in **3** (longer Δ) is probably a result of the stronger σ-donor capability of dppf.[8] The unusually large fold angle (FA) in [**4**]$^+$ likely arises from the steric congestion created by the phenyl rings of the tripod ligand, which causes the benzenoid ring of the indenyl ligand to twist upwards,

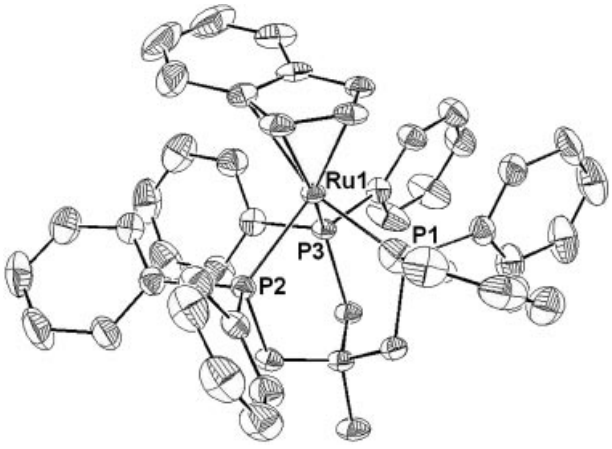

Figure 3. ORTEP diagram of [**4**]$^+$. Thermal ellipsoids are drawn to 50% probability level. Hydrogen atoms are omitted for clarity.

Table 1. Selected bond parameters of complexes **2**, **3**, [**4**]$^+$ and [CpRu(dppf)Cl].

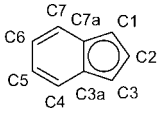

Complexes	**2**	**3**	[**4**]$^+$	[CpRu(dppf)Cl][14]
Δ [Å][a]	0.182(5)	0.193(4)	0.182(5)	–
Hinge angle (HA) [°][a]	7.43	7.69	7.71	–
Fold angle (FA) [°][a]	11.22	11.02	15.62	–
C*–Ru1[b]	1.913(5)	1.901(4)	1.973(5)	–
Ru1–P1	2.2568(14)	2.2556(9)	2.3120(13)	2.2858(14)
Ru1–P2	2.3160(14)	2.2959(9)	2.2479(14)	2.2844(13)
Ru1–P3	–	–	2.3170(13)	–
Ru1–Cl1	2.4194(14)	2.4434(9)		2.4443(13)
P1–Ru1–P2	96.71(5)	98.22(3)	88.81(5)	95.04(5)
P2–Ru1–P3	–	–	86.19(5)	–
P1–Ru1–P3	–	–	87.93(5)	–
P1–Ru1–Cl1	89.78(4)	90.99(3)	–	93.20(5)
P2–Ru1–Cl1	90.56(5)	90.43(3)	–	89.48(5)

[a] Slip-fold parameters as defined in ref.[15]. [b] C* = centroid of the five-membered ring, C1, C2, C3, C3a and C7a.

thereby increasing the FA. This steric congestion is also reflected in the significantly longer C*–Ru1 bond length.

The "ene" character of the "dangling" ethylindene substituent of **LH** in **2** was indicated by the short C3–C11 bond length [1.329(7) Å], of C–C double bond character.[16] The C–C bond lengths of the benzenoid ring have an average of 1.382 Å, consistent with aromaticity of the ring.[16]

The metric data for the structures of **2**, **3** and [**4**]$^+$ are significantly different from those of CpRu(dppf)Cl.[14] While the Ru1–P bond lengths in the latter complex are almost identical, the two Ru1–P bond lengths in each of **2**, **3** and [**4**]$^+$ differ substantially, by 0.04–0.07 Å, probably because of the steric repulsion between the benzenoid ring of the indenyl ligand and the phenyl rings bonded to P2, which are situated directly below the benzenoid ring. The Cp rings of dppf in **3** are almost eclipsed (synperiplanar), with a torsional angle (τ) of 4.3°, and the rings are tilted at an angle of 6.3°. The P1–Ru1–P2 angle of 98.22° is larger than those in **2** and [**4**]$^+$, undoubtedly because of the expanse of the dppf ligand. However, the value, like that of the Cp analogue (95.05°), falls in the range 91.6–102.2° reported for Ru(dppf) complexes.[17]

Synthesis of [(CpIInd)Ru(Josiphos)Cl]

Phosphane substitution of **1** or **1a** by the ferrocene-based chiral diphosphane ligand (*R*)-(–)-1-[(*S*)-2-(diphenylphosphanyl)ferrocenyl]ethyldicyclohexylphosphane {(*R*)-(*S*)-Josiphos} can likewise be achieved at an elevated temperature (Scheme 2). Because of the inequivalence of the two phosphorus atoms in (*R*)-(*S*)-Josiphos and the pseudotetrahedral geometry of **1** and **1a**, a pair of diastereomers is formed, as displacement of PPh_3 by chiral Josiphos generates a chiral ruthenium centre.

It was found that an 8-h reflux generated a 1:1:3:2 equilibrium mixture of **1**, free Josiphos, (*R*)-**5** and (*S*)-**5** diastereomers. Prolonged reaction time did not lead to completion, but gave instead a decomposition product with a ^{31}P NMR resonance at δ = 24.9 ppm. Pure (*R*)-**5** can be isolated by liquid chromatography of the mixture, with 'loss' of the (*S*)-**5** isomer. Purification by fractional crystallisation was rendered impossible by the similar solubility of **1** and **5**.

A similar reaction of **1a** with (*R*)-(*S*)-Josiphos (1:1) for 1.5 h gave a 1.5:1 molar mixture of (*R*)- and (*S*)-[CpRu(Josiphos)Cl] (**6**) diastereomers. Further heating caused epimerisation of (*S*)-**6** to (*R*)-**6**, with complete conversion in 8 h, indicating that (*S*)-**6** is the kinetic product, while (*R*)-**6** is the thermodynamically more stable isomer (Scheme 3). The simultaneous appearance of two new sets of doublets in the ^{31}P NMR spectrum, corresponding to (*R*)-**6** and (*S*)-**6**, respectively, indicated that the chelation of Josiphos was a concerted process. This was unlike the stepwise process observed in the analogous displacement reactions of **1a** by other chiral diphosphanes.[18]

Pure (*R*)-**6** can be isolated by either liquid chromatography or by fractional crystallisation. Isolation of pure (*S*)-**6** was in vain, owing to epimerisation to (*R*)-**6**, despite attempts to slow down the process by the presence of a free ligand (see rate studies below); the process was found to be accelerated on a silica-gel column.

The configuration at the metal centre of **5** was determined by matching the coupling constants of the pair of doublets observed in the ^{31}P NMR spectrum to those of **6** [structurally determined (*R*)-**6** possesses δ = 37.5 and 67.2 ppm ($^2J_{PP}$ = 53.4 Hz) and (*S*)-**6**: δ = 49.3 and 68.1 ppm ($^2J_{PP}$ = 49.6 Hz)]. Based on these, the resonances for the diastereoisomers of **5** were assigned as follows: a pair of

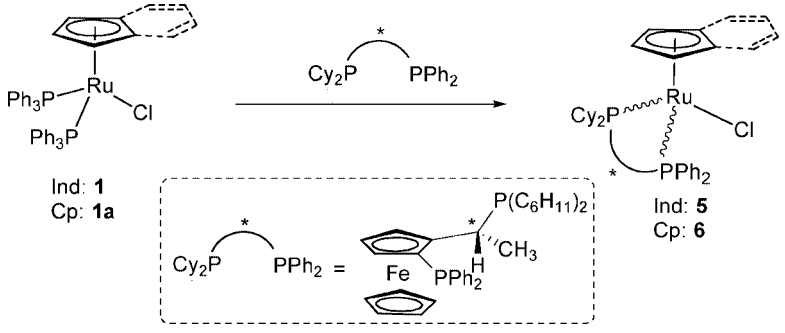

Scheme 2.

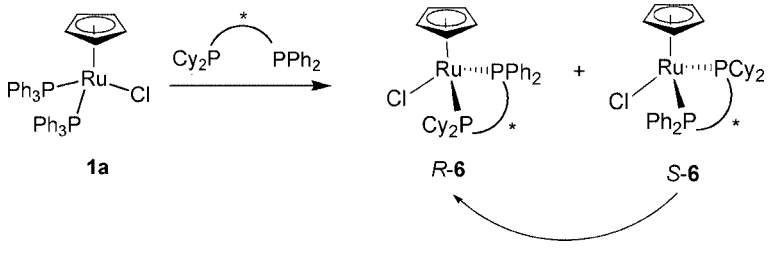

Scheme 3.

doublets at δ = 36.0 and 77.3 ppm ($^2J_{PP}$ = 53.4 Hz) for (*R*)-**5**, and δ = 60.5 and 68.4 ppm ($^2J_{PP}$ = 49.6 Hz) for (*S*)-**5**. In the ^{1}H NMR spectra of (*R*)-**5** and (*R*)-**6**, the cyclohexyl protons resonate as broad signals in the range δ = 0.6–2.7; the Me resonance sits on top of one of the broad signals. The Cp protons of Josiphos in (*R*)-**5** and (*R*)-**6** resonate in the range δ = 3.68–4.30. Protons signals at δ = 5.34 (H^1) and 5.73 ($H^{2,3}$) are assignable to protons of η^5-Ind in (*R*)-**5**. In (*R*)-**6**, the protons of η^5-CpRu are observed at δ = 4.49 ppm.

The NMR spectroscopic data of (*S*) isomers of **5** and **6** were obtained from spectra of their diastereoisomeric mixtures by eliminating the resonances assigned to their (*R*) isomers and the starting materials. The ^{31}P resonances of both (*S*)-**5** and (*S*)-**6** can be easily identified, as they are very well resolved. However, their ^{1}H resonances overlapped extensively with those of the corresponding (*R*) isomer, with the exception of the singlets at δ = 3.56 in (*S*)-**5** and 3.89 in (*S*)-**6**, which belong to the protons of the Cp ring of Josiphos.

The X-ray crystal structure of (*R*)-**6** was obtained. A view of the molecule is shown in Figure 4, together with selected bond parameters. The cyclopentadienyl ring is slightly distorted, with a hinge angle of 2.22° and Δ of 0.037 Å. The bond lengths of Ru1–P, Ru1–Cl1 and average Ru1–C (of Cp ring) are comparable to those of (*S*)-{RuCl(Cp)[(*R*)-dppp]}.[19] The longer Ru1–P2 compared to Ru1–P1 is also observed in the crystal structure of *trans*-$RuCl_2${(*R*)-(*S*)-Josiphos}$(py)_2$.[20]

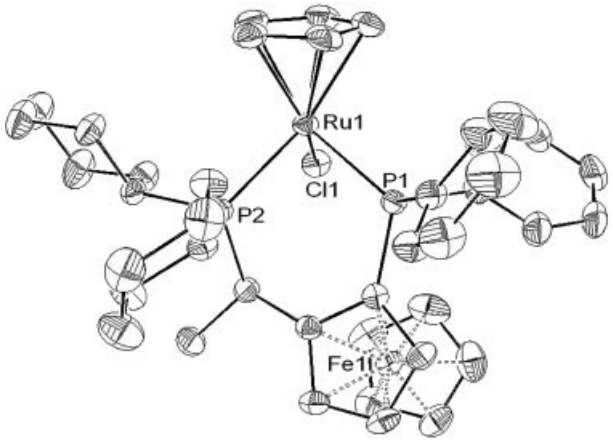

Figure 4. ORTEP diagram of (*R*)-**6**. Thermal ellipsoids are drawn to 50% probability level. Hydrogen atoms are omitted for clarity. Selected bond parameters: Δ = 0.037(4) Å; HA = 2.22°; C*–Ru1 1.858(4) Å; Ru1–P1 2.2804(11) Å; Ru1–P2 2.3115(11) Å; Ru1–Cl1 2.4525(11) Å; P1–Ru1–P2 90.22(4)°; P1–Ru1–Cl1 89.22(4)°; P2–Ru1–Cl1 90.41(4)°.

Epimerisation of 6

As both complexes **5** and **6** undergo $S \rightarrow R$ epimerisation, it would be desirable to investigate their configurational stability and racemisation processes, as these processes often determine the potential of chiral-at-metal complexes in homogeneous catalysis. Complex **6** was chosen to be investigated rather than **5**, as the latter is thermally unstable.

^{1}H and ^{31}P NMR spectral observations of the reaction of **1a** with Josiphos showed that the rate of epimerisation was markedly dependent on the concentration of free Josiphos in the reaction mixture. Thus, three experiments were carried out keeping Josiphos concentration [**J**] at 10 mM, and varying the molar ratio of **1a** to Josiphos. The results are given in Figure 5. In all three experiments, (*R*)-**6** and (*S*)-**6** were formed in about 1.2:1 ratio in the first 10 min of the reactions. Subsequently, the ratio of (*R*)-**6** to (*S*)-**6** increased rapidly in reactions **A** and **B**, as epimerisation proceeded at approximately similar rates, reaching a ratio of about 3 in 30 min, followed by a sharp increase to 118 at 90 min (reaction **A**), and 83.5 at 100 min (reaction **B**). It was observed that Josiphos was totally consumed at 30 min in reaction **A**, but was slowly consumed in reaction **B** to a negligible amount at about 50 min. In reaction **C**, using a 0.5 molar excess of Josiphos, epimerisation was observed to be extremely sluggish: the (*R*)-**6**/(*S*)-**6** ratio remained at about 1.5 up to 135 min, followed by a slow increase to about 10 in 500 min. This dramatic inhibition of epimerisation would suggest a dissociative type of mechanism, but the role of free Josiphos is currently still unclear to us. This case, involving a bidentate biphosphane, would not be expected to exactly parallel that for phosphane substitution in indenyl and $CpRu(PPh_3)_2$ complexes, for which a dissociative mechanism had been proposed by Gimeno on the basis of rate retardation by added PPh_3.[11] Nonetheless, the inhibitory effect of free Josiphos provides a useful way to control the rate of epimerisation.

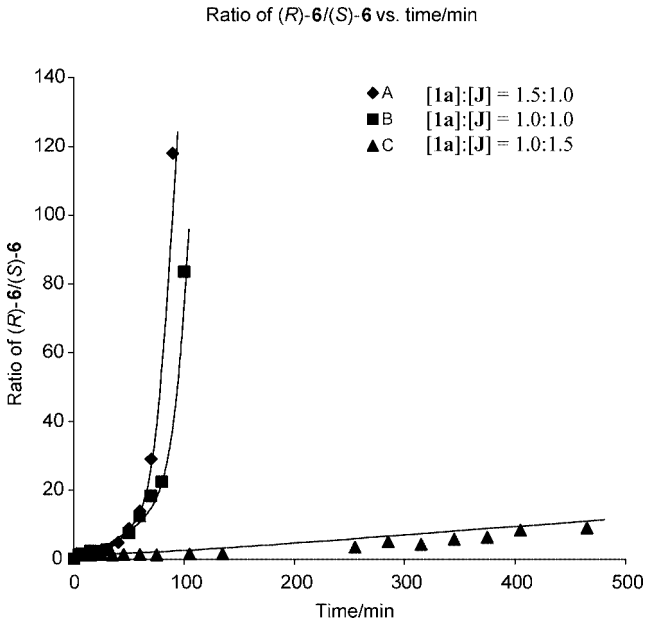

Figure 5. A plot of the ratio of (*R*)-**6**/(*S*)-**6** vs. time for the reaction of **1a** with Josiphos (**J**); [**J**] = 10 mM.

Complex (*R*)-**6** was observed to exhibit configurational stability in solution indefinitely, even at elevated temperature. As configurational stability is an asset for catalyst performance to give high enantioselectivity, (*R*)-**6** has good catalytic potential, especially for transfer hydrogenation of ketones, as was found for chiral-at-metal organoruthenium complexes.[21] Catalytic investigations of (*R*)-**6** are currently in progress in our laboratory.

Chloro Lability of [(Ind)Ru(dppf)Cl] (3)

As in the case of **1** and **1a**, chloro substitution of **3** provides a convenient pathway to new derivatives. It was found that chloride abstraction with $NaPF_6$ occurred readily in CH_3CN under reflux, giving the yellow acetonitrile solvento complex $[(Ind)Ru(dppf)(CH_3CN)]PF_6$ ([**7**]PF_6) (Scheme 4). This compound was fully characterised spectroscopically (see Experimental Section). The Cp protons of dppf display an ABCD pattern, similar to that in **3**.

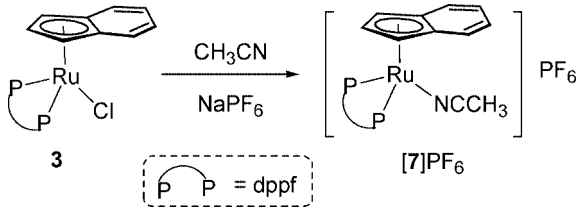

Scheme 4.

Treatment of **3** with NaN_3 in ethanol at reflux for 4 h afforded an 85% yield of **8** (Scheme 5), the spectral characteristics of which are given in Experimental Section. Here again, the Cp protons show an ABCD pattern.

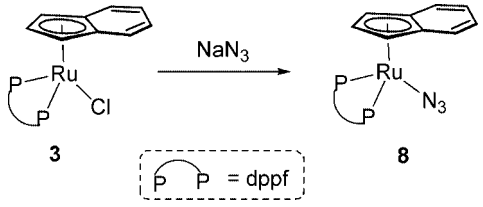

Scheme 5.

As at Pt^{II}[22] and Pd^{II}[23] centres, the azido ligand in **8** undergoes [3+2] dipolar cycloaddition reaction with dimethyl acetylenedicarboxylate, giving the N(2)-bound 4,5-bis(methoxycarbonyl)-1,2,3-triazolato complex **9** in 55% yield from an ambient temperature reaction (Scheme 6). Several cycloaddition reactions have been reported in half-sandwich ruthenium systems, like $[(Ind)Ru(LL)(N_3)]$, $[Cp^*Ru(LL)(N_3)]$ (LL = dppm, dppe)[10f] and $[CpRu(dppe)(N_3)]$.[24] This is a useful synthetic route to some heterocycles, but it should be noted that the viability of the method may be dependent on the substituents on the acetylenic carbons, as we found that the reaction of **8** with $(CN)_2C{\equiv}C(CN)_2$ or $HC{\equiv}C(CO_2Me)$ led to dissociation of the indenyl ligand and did not yield any isolable product.

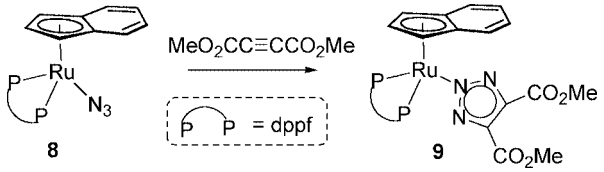

Scheme 6.

The ORTEP diagrams for the molecular structures of **8** and **9** are shown in Figures 6 and 7, respectively.

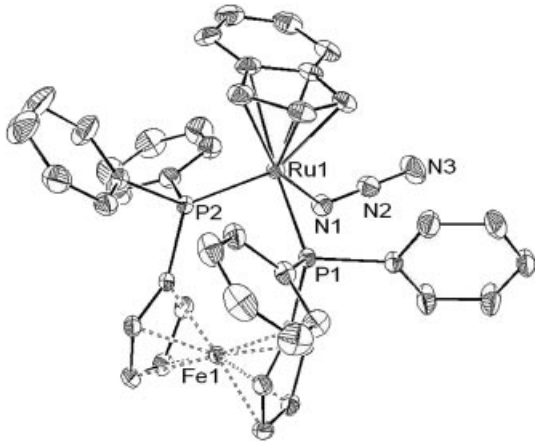

Figure 6. ORTEP diagram of **8**. Thermal ellipsoids are drawn to 50% probability level. Hydrogen atoms are omitted for clarity. Selected bond parameters: Δ = 0.163 Å; HA = 6.85°; FA = 8.70°; C*–Ru1 1.892 Å; Ru1–P1 2.2559(5) Å; Ru1–P 22.3251(6) Å; Ru–N1 2.1355(18) Å; N1–N2 1.192(3) Å; N2–N3 1.156(3) Å; P1–Ru1–P2 97.744(19)°; P1 Ru1–N1 84.42(5)°; P2–Ru1–N1 92.14(5)°; Ru1–N1–N2 117.96(15)°; N3–N2–N1 176.6(2)°.

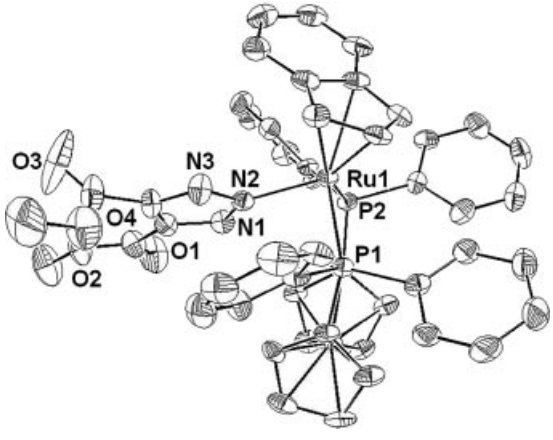

Figure 7. ORTEP diagram of **9**. Thermal ellipsoids are drawn to 50% probability level. Hydrogen atoms are omitted for clarity.

The slip-fold parameters of **8** fall in the normal range for η^5-coordination.[15] The Cp rings of the dppf ligand adopt a more stable synclinal staggered conformation, with tor-

Table 2. Selected bond lengths [Å] and angles [°] of **9** and [(Ind/Cp)Ru(dppe){$N_3C_2(CO_2Me)_2$}].

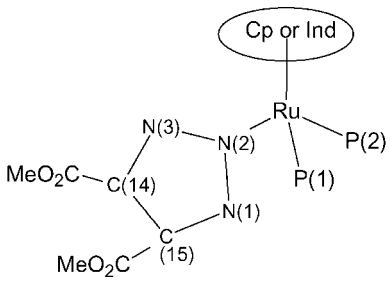

Complexes	**9**	[(Ind)Ru(dppe){$N_3C_2(CO_2Me)_2$}][10f]	[CpRu(dppe){$N_3C_2(CO_2Me)_2$}][24]
Δ [Å]	0.142	0.175	–
Hinge angle (HA) [°]	5.25	–	–
Fold angle (FA) [°]	9.63	–	–
C*–Ru1	1.909(8)	1.888(1)	–
Ru1–P1	2.3230(18)	2.2396(6)	–
Ru1–P2	2.2646(18)	2.2720(6)	–
Ru1–N2	2.070(6)	2.0904(18)	2.090(2)
N1–N2	1.306(8)	1.336(3)	1.331(3)
N2–N3	1.355(9)	1.336(3)	1.332(3)
N1–C15	1.352(10)	1.348(3)	1.351(3)
N3–C14	1.338(10)	1.351(3)	1.352(3)
C14–C15	1.385(11)	1.395(3)	1.400(4)
P1–Ru1–P2	98.08(6)	84.92(2)	85.13(3)
P1–Ru1–N2	91.35(17)	86.38(5)	86.48(6)
P2–Ru1–N2	87.54(16)	89.73(5)	89.89(6)
Ru1–N2–N1	126.4(5)	–	121.4(2)
Ru1–N2–N3	121.1(4)	–	125.2(2)
N1–N2–N3	112.2(6)	112.95(17)	113.4(2)
N2–N1–C15	106.8(6)	105.83(18)	105.6(2)
N2–N3–C14	105.3(6)	108.29(19)	105.5(2)
N1–C15–C14	107.2(6)	107.67(19)	107.7(2)
N3–C14–C15	108.5(7)	108.29(19)	107.8(2)

sional angle 39.09°. The Ru1–N1 bond length of 2.1355(18) Å falls within the range of reported values for azido Ru complexes.[25] The coordinated terminal azido ligand is almost linear, the N3–N2–N1 angle being 176.6°.

In **9**, Ru is coordinated to two phosphorus atoms of the dppf ligand, heterocycle $N_3C_2(CO_2Me)_2$ through N(2) and an η^5-indenyl ligand. The coordination geometry of **9** is effectively similar to those of its Ind/Cp analogues containing dppe.[10f,24] The only noticeable difference lies in the irregularity of the pentagonal heterocyclic ring in **9**. This undoubtedly is caused by the steric demands of the bulky dppf ligand. It is seen in the structure of **9** that the heterocycle is hemmed in by the phenyl rings of dppf; moreover, N3, being nearer to the benzenoid ring of the indenyl ligand, suffers from additional steric encumbrance, hence the shortened N2–N3 bond length.

Selected metric data of **9**, including the slip-fold distortion parameters, are listed in Table 2, which also gives the metric data of its Ind/Cp dppe analogues for comparison. While these analogues possess very similar bond parameters, these differ appreciably from those of **9**, especially the bond angles. These significant differences are no doubt a consequence of the bulkiness of the dppf ligand.

Conclusions

(Ind)Ru(PPh_3)$_2$Cl has been prepared and mono-, di- and trisubstitution derivatives have been obtained with the monophosphane ligand **LH**, dppf and triphos, respectively. (*R*) and (*S*) diastereomers have been obtained with Josiphos, but only the thermodynamically stable (*R*) isomer could be isolated pure. A similar result was obtained with CpRu(PPh_3)$_2$Cl. A rate study by ^{1}H NMR spectroscopy showed Josiphos-dependent epimerisation of CpRu(Josiphos)Cl. Chloro substitution of (Ind)Ru(dppf)Cl with CH_3CN and N_3^- appears to indicate that this process is as facile as in the well-studied complex CpRu(PPh_3)$_2$Cl. The [3+2] dipolar cycloaddition of the azido ligand provides an additional example for this uncommon occurrence at Ru.

Experimental Section

General: All reactions were carried out using conventional Schlenk techniques under inert nitrogen or under argon in an M. Braun Labmaster 130 Inert Gas System. NMR spectra were measured on a Bruker 300 FT NMR spectrometer; for ^{1}H and ^{31}P spectra, chemical shifts were referenced to residual H-signals of the deuterated

solvents C_6D_6, CD_3CN. IR spectra in KBr pellets were measured in the range 4000–400 cm^{-1} with a BioRad FTS-165 FTIR instrument. Mass spectra were run on a Finnigan Mat 95XL-T (FAB) or a Finnigan-MAT LCQ (ESI) spectrometer. Elemental analyses were performed by the microanalytical laboratory in-house. [(Ind)-$Ru(PPh_3)_2Cl$] (**1**)[7] and $C_9H_7(CH_2)_2PPh_2$[26] were prepared by the published methods. All other chemicals were obtained commercially and used without any further purification. All solvents were dried with sodium/benzophenone and distilled before use. Celite (Fluka AG), silica gel (Merck Kieselgel 60, 230–400 Mesh) were dried at 140 °C overnight before chromatographic use. Conventional numbering of indenyl protons is shown in Figure 8.

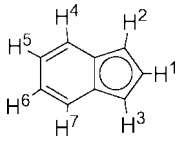

Figure 8. Numbering of indenyl protons.

Synthesis of [(Ind)Ru(PPh$_3$){Ph$_2$P(CH$_2$)$_2$C$_9$H$_7$}Cl] (2): $C_9H_7(CH_2)_2$-PPh_2 (35 mg, 0.11 mmol) was added to a red solution of **1** (70 mg, 0.09 mmol) in toluene (10 mL). The mixture was heated at 80 °C for 4 h. The resultant red solution was concentrated to about 1 mL and eluted through a silica gel column (2 × 2 cm) prepared in *n*-hexane with toluene/diethyl ether (10:1). From the red eluate, red microcrystals of [(Ind)Ru(PPh_3){$Ph_2P(CH_2)_2C_9H_7$}Cl] (**2**) (57 mg, 75% yield) were obtained upon recrystallisation from THF/hexane. X-ray diffraction-quality crystals were obtained from a concentrated ether solution with hexane layering after 2 d at –30 °C.

Data for 2: ^{1}H NMR (300 MHz, C_6D_6): δ = 1.73–1.90 (br. m, 1 H, C*H*$_2$), 2.18–2.30 (br. m, 1 H, C*H*$_2$), 2.93 (s, 2 H, C*H*$_2$ on IndH), 3.15 (s, 1 H, C*H*$_2$), 3.40–3.52 (m, 1 H, C*H*$_2$), 4.95–5.00 (m, 2 H, H^{2,3}), 5.78 (s, 1 H, H^1), 6.57–6.60 (d-like m, 1 H, IndH), 6.79–6.81, 6.84–6.94, 6.98–7.13, 7.19–7.22 (each m, total 29 H, H$^{4–7}$and Ph), 7.65–7.68 (d-like m, 1 H, Ph), 8.25 (t-like m, 2 H, Ph) ppm. ^{31}P{^{1}H} NMR: δ = 46.5, 50.0 [each d, $^2J_{PP}$ = 42.9 Hz, PPh_3 and IndH$(CH_2)_2$-PPh_2] ppm. FAB$^+$-MS: *m*/*z* (%) = 842 [M]$^+$, 808 [M – Cl]$^+$, 691 [M – Ind]$^+$, 581 [M – PPh_3]$^+$, 545 [M – PPh_3 – Cl]$^+$, 479 [M – IndH$(CH_2)_2PPh_2$ – Cl]$^+$, 429 [M – Ind – PPh_3 – Cl]$^+$. $C_{50}H_{43}ClP_2Ru$ (842.35): calcd. C 71.3, H 5.2; found C 71.6, H 5.3.

Synthesis of [(Ind)Ru(dppf)Cl] (3): 1,1′-Bis(diphenylphosphanyl)ferrocene (dppf) (0.76 g, 1.37 mmol) was added to a red solution of **1** (1 g, 1.29 mmol) in toluene (15 mL) and the mixture refluxed for 2 h. Red air- and moisture-stable crystalline solids, [(Ind)Ru(dppf)-Cl] **3**, precipitated out from the solution and were filtered (0.62 g, 60% yield). The supernatant was concentrated to about 5 mL. Addition of hexane (about 2 mL) gave a second crop after 2 h at 0 °C (0.27 g, 26% yield). In solution, the red compound of **3** decomposed in air within a day to a brown species. X-ray diffraction-quality crystals were obtained from a saturated solution of **3** in C_6D_6 after a day at room temperature.

Data for 3: ^{1}H NMR (300 MHz, C_6D_6): δ = 3.66, 3.83, 3.90 and 4.20 (each s, 2 H, C_5H_4), 4.66 (t, $^3J_{HH}$ = 2.5 Hz, 1 H, H^1), 5.57 (s, 2 H, H^{2,3}), 7.01–7.13 and 7.47–7.58 (m, 24 H, H$^{4–7}$ and Ph) ppm. ^{31}P{^{1}H} NMR: δ = 51.9 (s, dppf) ppm. FAB$^+$-MS: *m*/*z* (5) = 806 [M]$^+$, 771 [M – Cl]$^+$, 655 [M – Cl – Ind]$^+$. $C_{43}H_{35}ClFeP_2Ru$ (806.05): calcd. C 64.1, H 4.4; found C 64.3, H 4.1.

Synthesis of [(Ind)Ru(tripod)]PF$_6$ ([4]PF$_6$): $NaPF_6$ (20 mg, 0.12 mmol) and tripod (40 mg, 0.06 mmol) were added to a red solution of **1** (50 mg, 0.06 mmol) in toluene/THF (5:1, 12 mL). The mixture was refluxed for 4 h, during which the colour of the mixture changed from red to yellow. The resultant yellow suspension was filtered through Celite. The filtrate was concentrated to about 5 mL. Addition of ether (2 mL) gave yellow microcrystals, [(Ind)-Ru(tripod)]PF_6 ([**4**]PF_6), after 1 d at –30 °C (51 mg, 83% yield). X-ray diffraction-quality crystals were obtained from a saturated solution of [**4**]PF_6 in CH_2Cl_2 with ether layering after 2 d at –30 °C.

Data for [4]PF$_6$: ^{1}H NMR (300 MHz, CD_3CN): δ = 1.56–1.57 (m, 3 H, Me), 2.39 (br. s, 6 H, CH_2), 5.51 (d, $^3J_{HH}$ = 2.5 Hz, 2 H, H^{2,3}), 5.70 (t, $^3J_{HH}$ = 2.5 Hz, 1 H, H^1), 6.78–6.82 (br. s, 12 H, Ph), 7.04 (t, $^3J_{HH}$ = 7.4 Hz, 12 H, Ph), 7.22 (t, $^3J_{HH}$ = 7.4 Hz, 6 H, Ph), 7.31–7.34 and 7.43–7.47 (each m, 2 H, H$^{4–7}$) ppm. ^{31}P{^{1}H} NMR: δ = 39.9 (s, tripod), –142.9 (septet, PF_6) ppm. IR (KBr): $\tilde{\nu}$ = 058 (w), 2923 (w), 2868 (w), 1482 (w), 1434 (m), 1092 (m), 839 [vs. (PF_6)], 744 (m), 697 (s), 557 [m (PF_6)], 517 (s) cm^{-1}. FAB$^+$-MS: *m*/*z* (%) = 841 [M]$^+$. FAB$^–$-MS: *m*/*z* (%) = 145 [PF_6]$^–$. $C_{50}H_{46}F_6P_4Ru$ (985.86): calcd. C 60.9, H 4.7; found C 60.5, H 5.2.

Synthesis of [(Ind)Ru{(*R*)-(*S*)-Josiphos}Cl] (5): (*R*)-(–)-1-[(*S*)-2-(Diphenylphosphanyl)ferrocenyl]ethyldicyclohexylphosphane {(*R*)-(*S*)-Josiphos} (23 mg, 0.04 mmol) was added to a red solution of **1** (30 mg, 0.04 mmol) in toluene (5 mL) and the mixture was refluxed. The reaction was monitored using ^{31}P NMR spectroscopy. Refluxing was ceased when the ratio of starting materials and product remained constant (about 8 h). The solution was concentrated to about 2 mL and loaded onto a silica gel column (2 × 8 cm) prepared in *n*-hexane. Elution gave three fractions: (i) a yellow eluate in hexane/diethyl ether (1:1, about 4 mL), which recovered free (*R*)-(*S*)-Josiphos (2 mg, 9% recovery); (ii) an orange-red solution in hexane/diethyl ether (1:1, about 15 mL), which yielded [(*R*)-(Ind)-Ru{(*R*)-(*S*)-Josiphos}Cl] [(*R*)-**5**] (12 mg, 37% yield) as orange solids; and (iii) a red solution in THF (about 3 mL), which recovered unreacted **1** (2 mg, 7% recovery).

Data for (*R*)-5: ^{1}H NMR (300 MHz, C_6D_6): δ = 0.87–1.10 (br. m, 6 H, Cy), 1.24–1.56 (br. m) with 1.47 (dd, sitting on top of br. m, $^3J_{HH}$ = 7.41, $^2J_{HP}$ = 9.9 Hz, total 11 H, Cy and Me), 1.63–1.68 (br. m, 1 H, Cy), 1.76–1.85 (br. m, 2 H, Cy), 1.94–1.98 (br. m, 2 H, Cy), 2.18–2.32, 2.37–2.50 and 2.60–2.68 (each br. m, 1 H, Cy), 3.68 (s, 5 H, Cp), 4.06 (t-linked m, 1 H, Cp), 4.19 and 4.23 (each br. s, 1 H, Cp), 5.22–5.29 [m, 1 H, C*H*MeP(Cy)$_2$], 5.34 (s, 1 H, H^1), 5.73 (s, 2 H, H^{2,3}), 6.89–6.94, 6.99–7.08, 7.11–7.16, 7.24–7.30, 7.44–7.49, 7.52–7.59 and 7.75–7.78 (each m, total 14 H, H$^{4–7}$ and Ph) ppm. ^{31}P{^{1}H} NMR: δ = 36.0 (d, $^2J_{PP}$ = 53.4 Hz, Josiphos), 77.3 (d, $^2J_{PP}$ = 53.4 Hz, Josiphos) ppm. FAB$^+$-MS: *m*/*z* (%) = 846 [M]$^+$, 812 [M – Cl]$^+$. $C_{45}H_{51}ClFeP_2Ru$ (846.20): calcd. C 63.9, H 6.1; found C 63.9, H 6.3.

Synthesis of [CpRu{(*R*)-(*S*)-Josiphos}Cl] (6): (*R*)-(*S*)-Josiphos (18 mg, 0.03 mmol) was added to a yellow solution of **1a** (30 mg, 0.04 mmol) in toluene (5 mL) and the mixture was refluxed for 8 h. The solvent was removed in vacuo and the residue extracted using ether (3 × 2 mL).

Purification Method (i): The ether extract was concentrated to about 1 mL and loaded onto a silica gel column (2 × 4 cm) prepared in *n*-hexane. Elution gave two fractions: (i) a yellow eluate in hexane/diethyl ether (5:1, about 20 mL), which yielded [(*R*)-CpRu{(*R*)-(*S*)-Josiphos}Cl] [(*R*)-**6**] (28 mg, 85% yield) as orange microcrystals; and (ii) a yellow solution in hexane/diethyl ether (1:1, about 3 mL), which gave unreacted **1a** (6 mg, 20% recovery).

Purification Method (ii): The ether extract was concentrated to about 1 mL and hexane was added (about 2 mL). Orange solids of **1a** were recovered after 1 d at –30 °C, and removed by filtration (5 mg, 16% recovery). The mother liquor was concentrated to about 1 mL and hexane was added (about 4 mL). Orange yellow

solids of (*R*)-**6** were obtained after 1 d at –30 °C (15 mg, 46% yield). Subsequently, four additional crops of (*R*)-**6** were obtained, each about 3 mg (total 11 mg, 34% yield). X-ray diffraction-quality crystals were obtained from a concentrated ether solution with hexane layering after a day at –30 °C.

Data for (*R*)-6: ^{1}H NMR (300 MHz, C_6D_6): δ = 0.61–0.77 (br. m, 2 H, Cy), 1.29–1.55 (br. m) with 1.52 (dd, sitting on top of br. m, $^3J_{HH}$ = 7.41, $^2J_{HP}$ = 9.06 Hz, total 13 H, Cy and Me), 1.65–1.92 (br. m, 6 H, Cy), 2.09–2.18 and 2.41–2.46 (each br. m, 2 H, Cy), 3.79 (s, 5 H, Cp), 4.11 (t, $^3J_{HH}$ = 2.49 Hz, 1 H, Cp), 4.27 and 4.30 (each br. s, 1 H, Cp), 4.49 (s, 5 H, η^5-*Cp*Ru), 5.23–5.34 [m, 1 H, C*H*MeP(Cy)$_2$], 6.85–6.90 and 7.20–7.23 (each m, 1 H, Ph), 6.93–6.97, 7.01–7.06 and 7.31–7.36 (each m, 2 H, Ph), 8.71 (br. s, 2 H, Ph) ppm. ^{31}P{^{1}H} NMR: δ = 37.5 (d, $^2J_{PP}$ = 53.4 Hz, Josiphos), 67.2 (d, $^2J_{PP}$ = 53.4 Hz, Josiphos) ppm. FAB$^+$-MS: *m*/*z* (%) = 846 [M]$^+$, 812 [M – Cl]$^+$. $C_{41}H_{49}ClFeP_2Ru\cdot(CH_3CH_2)_2O$ (870.26): calcd. C 62.1, H 6.8; found C 62.2, H 6.8.

Epimerisation Kinetics: Complex **1a** [2.4 mg, 3.3 mmol (reaction **A**); 3.6 mg, 5 mmol (reaction **B**); 5.4 mg, 7.5 mmol (reaction **C**)] and (*R*)-(*S*)-Josiphos (3.0 mg, 5.0 mmol) were added to three different NMR tubes in three different ratios, that is, 1:1.5, 1:1 and 1.5:1. [D$_8$]toluene (0.5 mL) was added into each NMR tube. The initial ^{1}H and ^{31}P NMR spectrum of each reaction mixture was measured, and then at intervals during the reaction at 100 °C. The concentration of each component in the reaction mixtures was obtained from the integration of the Cp protons of the Josiphos [δ = 3.71 in (*R*)-**6** and δ = 3.89 in (*S*)-**6**], using as internal standard the residual 0.1% H-signal of 99.9% [D$_8$]toluene.

Synthesis of [(Ind)Ru(dppf)(CH$_3$CN)]PF$_6$ ([7]PF$_6$): $NaPF_6$ (16 mg, 0.09 mmol) was added to a red suspension of **3** (50 mg, 0.06 mmol) in CH_3CN (10 mL) and the mixture was refluxed. The colour of the suspension changed slowly from red to yellow in 4 h. The suspension was filtered and the filtrate was evacuated to dryness. The residue was redissolved in THF (about 4 mL) and hexane (about 2 mL) was added. Yellow crystals of [(Ind)Ru(dppf)(CH$_3$CN)]PF$_6$ ([7]PF$_6$) (55 mg, 93% yield) were obtained after 1 d at –30 °C.

Data for [7]PF$_6$: ^{1}H NMR (300 MHz, $CDCl_3$): δ = 2.15 (s, 3 H, C*H*$_3$CN), 4.22, 4.33 and 4.35 (each s, 2 H, C_5H_4), 4.44 (br. s, 3 H, C_5H_4 and H^1), 4.60 (d, $^3J_{HH}$ = 2.5 Hz, 2 H, H^{2,3}), 6.63–6.66 and 7.18–7.21 (each 4-line m, 2 H, H$^{4–7}$), 6.82–6.88, 7.28–7.33, 7.40–7.52 (m, 20 H, Ph) ppm. ^{31}P{^{1}H} NMR: δ = 50.7 (s, dppf), –144.1 (septet, PF_6) ppm. IR (KBr): $\tilde{\nu}$ = 055 (w), 2974 (w), 2057 (w), 2276 [w (CN)], 1481 (m), 1435 (m), 1158 (m), 1092 (m), 840 [vs. (PF_6)], 749 (s), 699 (s), 557 [s (PF_6)], 514 (m) cm^{-1}. FAB$^+$-MS: *m*/*z* (%) = 812 [M]$^+$, 771 [M – CH_3CN]$^+$, 655 [M – CH_3CN – C_9H_7]$^+$. FAB$^-$-MS: *m*/*z* (%) = 145 [PF_6]$^-$. $C_{45}H_{38}F_6FeNP_3Ru\cdot$½$CH_3CN$ (977.16): calcd. C 56.5, H 4.0, N 2.2; found C 56.0, H 3.9, N 2.1.

Synthesis of [(Ind)Ru(dppf)N$_3$] (8): NaN_3 (20 mg, 0.3 mmol) was added to a red suspension of **3** (50 mg, 0.06 mmol) in EtOH (10 mL) and the mixture was refluxed for 4 h. The solvent was removed in vacuo and the red residue extracted using CH_2Cl_2 (2 × 4 mL). The extract was concentrated to about 3 mL and hexane (about 10 mL) was added. After being kept overnight at –30 °C, red crystals of [(Ind)Ru(dppf)N$_3$] **8** (43 mg, 85% yield) were obtained. X-ray diffraction-quality crystals were obtained from a saturated solution in CH_2Cl_2 with hexane layering after 2 d at –30 °C.

Data for 8: ^{1}H NMR (300 MHz, C_6D_6): δ = 3.79, 4.05, 4.21 and 4.29 (each s, 2 H, C_5H_4), 4.58 (s, 1 H, H^1), 4.79 (s, 2 H, H^{2,3}), 7.09–7.12, 7.14–7.23, 7.26–7.29, 7.39–7.44, 7.47–7.52 (each m, total 24

Table 3. Crystal and structure refinement data.

	2	**3**	[**4**]PF$_6$
Formula	$C_{54}H_{53}ClOP_2Ru$	$C_{43}H_{35}ClFeP_2Ru$	$C_{51.5}H_{49}Cl_3F_6P_4Ru$
Formula mass	916.42	806.02	1113.21
Space group	$P2_1/c$	$P2_1/c$	$P\bar{1}$
Crystal system	monoclinic	monoclinic	triclinic
Unit cell dimensions			
a [Å]	12.433(5)	11.5291(5)	12.5364(5)
b [Å]	15.543(6)	29.8651(15)	13.2396(5)
c [Å]	23.785(9)	11.3638(5)	15.9901(6)
α [°]	90	90	98.356(1)
β [°]	101.836(10)	118.9740(10)	103.723(1)
γ [°]	90	90	92.325(1)
Cell volume [Å^3]	4499(3)	3423.0(3)	2543.08(17)
Z	4	4	2
D_{calcd} [g cm^{-3}]	1.353	1.564	1.454
Absorption coefficient [mm^{-1}]	0.518	1.069	0.648
F(000) electrons	1904	1640	1134
Crystal size [mm^3]	0.16 × 0.09 × 0.09	0.28 × 0.14 × 0.08	0.22 × 0.12 × 0.04
θ range for data collection [°]	2.13–25.00	2.02–27.50	2.20–26.37
Index ranges	$-14 \le h \le 14$	$-12 \le h \le 14$	$-15 \le h \le 15$
	$-18 \le k \le 17$	$-28 \le k \le 38$	$-16 \le k \le 16$
	$-28 \le l \le 16$	$-14 \le l \le 14$	$0 \le l \le 19$
Reflections collected	26102	24177	36189
Independent reflections	7923	7849	10372
Max. and min. transmission	0.9549 and 0.9217	0.9194 and 0.7540	0.9745 and 0.8705
Data/restraints/parameters	7923/0/532	7849/0/433	10372/18/612
Gof	0.980	1.095	1.038
Final *R* indices [$I > 2\sigma(I)$]	R_1 = 0.0542	R_1 = 0.0491	R_1 = 0.0648
	wR_2 = 0.0965	wR_2 = 0.0981	wR_2 = 0.1862
R indices (all data)	R_1 = 0.1004	R_1 = 0.0649	R_1 = 0.0845
	wR_2 = 0.1097	wR_2 = 0.1037	wR_2 = 0.2032
Largest diff. peak and hole [e Å^{-3}]	0.565 and –0.400	0.738 and –0.500	2.127 and –0.421

Table 4. Crystal and structure refinement data.

	(*R*)-**6**	**8**	**9**
Formula	$C_{43}H_{54}ClFeO_{0.50}P_2Ru$	$C_{43}H_{35}FeN_3P_2Ru$	$C_{51.50}H_{46}Cl_5FeN_3O_4P_2Ru$
Formula mass	833.17	897.53	1167.02
Space group	$P2_12_12_1$	$P2_1/n$	$P2_1/c$
Crystal system	orthorhombic	monoclinic	monoclinic
Unit cell dimensions			
a [Å]	9.546(2)	11.3220(3)	17.8241(14)
b [Å]	20.204(4)	14.5824(3)	11.6367(10)
c [Å]	21.200(4)	23.3452(5)	25.689(2)
α [°]	90	90	90
β [°]	90	96.5650(10)	103.167(2)
γ [°]	90	90	90
Cell volume [Å^3]	4088.9(15)	3829.06(16)	5188.2(7)
Z	4	4	4
D_{calcd} [g cm^{-3}]	1.353	1.557	1.494
Absorption coefficient [mm^{-1}]	0.897	1.034	0.937
F(000) electrons	1732	1824	2372
Crystal size [mm^3]	0.30 × 0.22 × 0.10	0.34 × 0.20 × 0.10	0.32 × 0.18 × 0.14
θ range for data collection [°]	2.02–30.51	2.10–26.37	2.11–26.37
Index ranges	$-13 \le h \le 13$	$-14 \le h \le 14$	$-22 \le h \le 21$
	$0 \le k \le 28$	$0 \le k \le 18$	$0 \le k \le 14$
	$0 \le l \le 30$	$0 \le l \le 29$	$0 \le l \le 32$
Reflections collected	61668	35653	42001
Independent reflections	11860	7793	10631
Max. and min. transmission	0.9156 and 0.7746	0.9037 and 0.7201	0.8800 and 0.7537
Data/restraints/parameters	11860/2/434	7793/0/478	10631/28/625
Gof	1.199	1.056	1.137
Final *R* indices [$I > 2\sigma(I)$]	R_1 = 0.0484	R_1 = 0.0450	R_1 = 0.0881
	wR_2 = 0.1292	wR_2 = 0.1091	wR_2 = 0.2225
R indices (all data)	R_1 = 0.0535	R_1 = 0.0569	R_1 = 0.1148
	wR_2 = 0.1322	wR_2 = 0.1159	wR_2 = 0.2373
Largest diff. peak and hole [e Å^{-3}]	1.004 and –0.498	1.345 and –1.054	1.925 and –1.013

H, H$^{4-7}$ and Ph) ppm. $^{31}P\{^1H\}$ NMR: δ = 52.5 (s, dppf) ppm. IR (KBr): $\tilde{\nu}$ = 053 (w), 2025 [vs. (N_3)], 1433 (w), 1159 (w), 1091 (w), 1034 (w), 745 (m), 697 (m), 513 (m) cm^{-1}. FAB$^+$-MS: *m*/*z* (%) = 785 [M – N_2]$^+$, 771 [M – N_3]$^+$, 670 [M – Ind – N_2]$^+$, 655 [M – Ind – N_3]$^+$. $C_{43}H_{35}FeN_3P_2Ru$ (812.62): calcd. C 63.6, H 4.3, N 5.2; found C 63.5, H 4.8, N 5.2.

Synthesis of [(Ind)Ru(dppf){$N_3C_2(CO_2Me)_2$}] (9): Dimethyl acetylenedicarboxylate (38 μL, 0.31 mmol) was added into a red solution of **8** (50 mg, 0.06 mmol) in CH_2Cl_2 (10 mL) and the reaction mixture was stirred at room temperature for 24 h. The colour of the solution slowly changed from red to orange-red. The solution was concentrated to about 2 mL and hexane (8 mL) was added. Yellow crystals [(Ind)Ru(dppf){$N_3C_2(CO_2Me)_2$}] **9** (33 mg, 55% yield) were obtained after 18 h at –10 °C. X-ray diffraction-quality crystals were obtained from a saturated solution in CH_2Cl_2 with ether layering after 1 week at 4 °C.

Data for 9: ^{1}H NMR (300 MHz, C_6D_6): δ = 3.52 (s, 6 H, Me), 3.76, 4.10, 4.31 and 4.34 (each s, 2 H, C_5H_4), 4.78 (s, 1 H, H^1), 5.35 (s, 2 H, H^{2,3}), 6.86–6.90 (m, 2 H, H$^{4-7}$), 6.96–6.97, 7.16–7.43, 7.72–7.78 (each m, total 22 H, H$^{4-7}$ and Ph) ppm. $^{31}P\{^1H\}$ NMR: δ = 56.8 (s, dppf) ppm. IR (KBr): $\tilde{\nu}$ = 057 (w), 2945 (w), 1736 [vs. (C=O)], 1434 [m (N=N)], 1292 [m (C–O)], 1165 (m), 1087 (s), 772 (m), 697 (m), 508 (m) cm^{-1}. FAB$^+$-MS: *m*/*z* 955 [M]$^+$, 771 [M – $N_3C_2(CO_2Me)_2$]$^+$. $C_{49}H_{41}FeN_3O_4P_2Ru$ (954.73): calcd. C 61.6, H 4.3, N 4.4; found C 61.7, H 3.8, N 4.4.

Crystal Structure Determinations: Crystals were mounted on quartz fibres. X-ray data were collected on a Bruker AXS APEX system, using Mo-K_α radiation, with the SMART suite of programs.[27] Data were processed and corrected for Lorentz and polarisation effects with SAINT,[28] and for absorption effects with SADABS.[29] Structural solution and refinement were carried out with the SHELXTL suite of programs.[30] Crystal and structure refinement data are summarised in Tables 3 and 4. The structures were solved by direct methods or Patterson maps to locate the heavy atoms, followed by difference maps for the light, non-hydrogen atoms. All non-hydrogen atoms were generally given anisotropic displacement parameters in the final model.

CCDC-616431 to -616436 contain the supplementary crystallographic data for this paper. These data can be obtained free of charge from The Cambridge Crystallographic Data Centre via www.ccdc.cam.ac.uk/data_request/cif.

Acknowledgments

The authors acknowledge with thanks support from the Academic Research Fund (grant no. 143-000-209-112) to L. Y. G., Institute of Chemical and Engineering Sciences for a research scholarship to S. Y. N. and technical assistance from Dr. L. L. Koh and Ms. G. K. Tan for X-ray structure determinations of **2** and **3**.

[1] See for instance the following: a) C. A. Tolman, *Chem. Rev.* **1977**, *77*, 313; b) D. J. Darensbourg, A. H. Graves, *Inorg. Chem.* **1979**, *18*, 1257; c) J. D. Atwood, M. J. Wovkulich, D. C. Sonnenberger, *Acc. Chem. Res.* **1983**, *16*, 350; d) R. L. Harlow, R. J. McKinney, J. F. Whitney, *Organometallics* **1983**, *2*, 1839; e) A. G. Orpen, N. G. Connelly, *J. Chem. Soc., Chem. Commun.* **1985**, 1310.

[2] See for instance the following: a) L. Dahlenburg, *Coord. Chem. Rev.* **2005**, *249*, 2962; b) N. Mézailles, L. Ricard, F. Gagosz, *Org. Lett.* **2005**, *7*, 4133; c) A. D. Phillips, L. Gonsalvi, A. Romerosa, F. Vizza, M. Peruzzini, *Coord. Chem. Rev.* **2004**, *248*,

955; d) S. R. Klei, T. D. Tilley, R. G. Bergman, *Organometallics* **2002**, *21*, 4905; e) D. Ferraris, B. Young, T. Dudding, T. Lectka, *J. Am. Chem. Soc.* **1998**, *120*, 4548; f) J. P. Wolfe, S. Wagaw, S. L. Buchwald, *J. Am. Chem. Soc.* **1996**, *118*, 7215.
[3] J. D. Gilbert, G. Wilkinson, *J. Chem. Soc. A* **1969**, 1749.
[4] a) S. G. Davies, J. P. McNally, A. J. Smallridge, *Adv. Organomet. Chem.* **1990**, *30*, 1; b) T. Blackmore, M. I. Bruce, F. G. A. Stone, *J. Chem. Soc. A* **1971**, 2376; c) M. I. Bruce, N. J. Windsor, *Aust. J. Chem.* **1977**, *30*, 1601; d) G. S. Ashby, M. I. Bruce, I. B. Tomkins, R. C. Wallis, *Aust. J. Chem.* **1979**, *32*, 1003; e) M. I. Bruce, F. S. Wong, B. W. Skelton, A. H. White, *J. Chem. Soc., Dalton Trans.* **1981**, 1398; f) M. I. Bruce, M. G. Humphery, J. M. Patrick, A. H. White, *Aust. J. Chem.* **1983**, *36*, 2065.
[5] a) V. Cadierno, P. Crochet, S. E. García-Carrido, J. Gimeno, *Dalton Trans.* **2004**, 3635; b) Y. Wakatsuki, M. Tokunaga, *Angew. Chem. Int. Ed. Engl.* **1998**, *37*, 2867; c) D. B. Grotjahn, D. A. Lev, *J. Am. Chem. Soc.* **2004**, *126*, 12232; d) Y. Wakatsui, M. Tokunaga, T. Suzuki, *Org. Lett.* **2001**, *3*, 735; e) Y. Wakatsuki, A. Horiuchi, *J. Am. Chem. Soc.* **2001**, *123*, 11917.
[6] a) K.-S. Gan, T. S. A. Hor in *Ferrocenes: Homogeneous Catalysis, Organic Synthesis and Materials Science* (Eds.: A. Togni, T. Hayashi), Wiley-VCH, Weinheim, Germany, **1995**, p. 3; b) H.-U. Blaser, W. Brieden, B. Pugin, F. Spindler, M. Studer, A. Togni, *Top. Catal.* **2002**, *19*, 3.
[7] L. A. Oro, M. A. Ciriano, M. Campo, *J. Organomet. Chem.* **1985**, *289*, 117.
[8] V. Cadierno, J. Díez, M. P. Gamasa, J. Gimeno, E. Lastra, *Coord. Chem. Rev.* **1999**, *193–195*, 147 and references cited therein.
[9] See for example the following and references cited therein: a) J. Díez, M. P. Gamasa, J. Gimeno, E. Lastra, A. Villar, *Organometallics* **2005**, *24*, 1410; b) S. Conejero, J. Díez, M. P. Gamasa, J. Gimeno, *Organometallics* **2004**, *23*, 6299; c) M. Bassetti, P. Alvarez, J. Gimeno, E. Lastra, *Organometallics* **2004**, *23*, 5127; d) P. Alvarez, E. Lastra, J. Gimeno, M. Bassetti, L. R. Falvello, *J. Am. Chem. Soc.* **2003**, *125*, 2386; e) V. Cadierno, M. P. Gamasa, J. Gimeno, C. González-Bernardo, E. Pérez-Carreño, S. García-Granda, *Organometallics* **2001**, *20*, 5177.
[10] a) K. M. Rao, E. K. Rymmai, *Polyhedron* **2003**, *22*, 307; b) S. S. Keisham, Y. A. Mozharivskyj, P. J. Carroll, M. R. Kollipara, *J. Organomet. Chem.* **2004**, *689*, 1249; c) K. S. Singh, G. P. A. Yap, K. A. Kreisel, M. R. Kollipara, *J. Coord. Chem.* **2005**, *58*, 1607; d) P. Govindaswamy, C. Sinha, M. R. Kollipara, *J. Organomet. Chem.* **2005**, *690*, 3465; e) K. S. Singh, Y. A. Mozahrivskyj, C. Thöne, M. R. Kollipara, *J. Organomet. Chem.* **2005**, *690*, 3720; f) K. S. Singh, C. Thöne, M. R. Kollipara, *J. Organomet. Chem.* **2005**, *690*, 4222; g) K. S. Singh, C. Thöne, M. R. Kollipara, *J. Coord. Chem.* **2006**, *59*, 333.
[11] M. P. Gamasa, J. Gimeno, C. Gonzalez-Bernardo, B. M. Martin-Vaca, D. Monti, M. Bassetti, *Organometallics* **1996**, *15*, 302.
[12] J. J. Bishop, A. Davison, *Inorg. Chem.* **1971**, *10*, 826.
[13] a) D. Gareau, C. Sui-Seng, L. F. Groux, F. Brisse, D. Zargarian, *Organometallics* **2005**, *24*, 4003; b) D. Zargarian, *Coord. Chem. Rev.* **2002**, *233–234*, 157.
[14] X. L. Lu, Ph.D Thesis, National University of Singapore, Singapore, **2002**.
[15] For indenyl complexes containing undistorted η^5 rings: Δ = 0.03 Å, HA = 2.5°, FA = 4.4°; for those containing distorted η^5 rings: Δ = 0.11–0.42 Å, HA = 7–14°, FA = 6–13°; and for those wherein the five-membered ring is η^3-coordinated: Δ = 0.8 Å, FA = 28°. See: A. K. Kakkar, N. J. Taylor, T. B. Marder, J. K. Shen, N. Hallinan, F. Basolo, *Inorg. Chim. Acta* **1992**, *198–200*, 219.
[16] L. Pauling, *The Nature of the Chemical Bond*, Cornell University Press, Ithaca, NY, **1960**, chapter 7, p. 221.
[17] G. Bandoli, A. Dolmella, *Coord. Chem. Rev.* **2000**, *209*, 161.
[18] G. Consiglio, F. Morandini, F. Bangerter, *Inorg. Chem.* **1982**, *21*, 455.
[19] F. Morandini, G. Consiglio, B. Straub, G. Ciani, A. Sironi, *J. Chem. Soc., Dalton Trans.* **1983**, 2293.
[20] C. G. Leong, O. M. Akotsi, M. J. Ferguson, S. H. Bergens, *Chem. Commun.* **2003**, 750.
[21] J.-B. Sortais, V. Ritleng, A. Voelklin, A. Holuigue, H. Smail, L. Barloy, C. Sirlin, G. K. M. Verzijl, J. A. F. Boogers, A. H. M. de Vries, J. G. de Vries, M. Pfeffer, *Org. Lett.* **2005**, *7*, 1247.
[22] a) W. Beck, K. Schropp, *Chem. Ber.* **1975**, *108*, 3317; b) W. P. Fehlhammer, L. F. Dahl, *J. Am. Chem. Soc.* **1972**, *94*, 3370.
[23] T. Kemmerich, J. H. Nelson, N. E. Takach, H. Boeheme, B. Jablonski, W. Beck, *Inorg. Chem.* **1982**, *21*, 1226.
[24] C. W. Chang, G. H. Lee, *Organometallics* **2003**, *22*, 3107 and references cited therein.
[25] P. Govindaswamy, P. J. Carroll, Y. A. Mozharivskyj, M. R. Kollipara, *J. Organomet. Chem.* **2005**, *690*, 885.
[26] Y. Kataoka, Y. Iwato, T. Yamagata, K. Tani, *Organometallics* **1999**, *18*, 5423.
[27] *SMART* version 5.628, Bruker AXS Inc., Madison, WI, USA, **2001**.
[28] *SAINT*+ version 6.22a, Bruker AXS Inc., Madison, WI, USA, **2001**.
[29] G. M. Sheldrick, *SADABS*, University of Göttingen, Germany, **1996**.
[30] *SHELXTL* version 5.1, Bruker AXS Inc., Madison, WI, USA, **1997**.

Received: August 3, 2006
Published Online: November 28, 2006

